Geotail observations of plasma sheet ion composition over 16 years: On variations of average plasma ion mass and O+ triggering substorm model

AUTHOR(S):

Nosé, Masahito; Ieda, A.; Christon, S. P.

CITATION:

Nosé, Masahito ...[et al]. Geotail observations of plasma sheet ion composition over 16 years: On variations of average plasma ion mass and O+ triggering substorm model. Journal of Geophysical Research A: Space Physics 2009, 114(7): A07223.

ISSUE DATE:

2009

URL:

http://hdl.handle.net/2433/91251

JOURNAL OF GEOPHYSICAL RESEARCH, VOL. , XXXX, DOI:10.1029/,

Geotail observations of plasma sheet ion composition over 16 years: On variations of average plasma ion mass and O^+ triggering substorm model

M. Nosé

Data Analysis Center for Geomagnetism and Space Magnetism, Graduate School of Science, Kyoto University, Kyoto, Japan.

A. Ieda

Solar-Terrestrial Environment Laboratory, Nagoya University, Nagoya, Aichi, Japan.

S. P. Christon

Focused Analysis and Research, Columbia, Maryland, USA.

Abstract.

We examined long-term variations of ion composition in the plasma sheet, using energetic (9.4-212.1 keV/*e*) ion flux data obtained by the suprathermal ion composition spectrometer (STICS) sensor of the energetic particle and ion composition (EPIC) instrument onboard the Geotail spacecraft. EPIC/STICS observations are available from 17 October 1992 for more than 16 years, covering the declining phase of solar cycle 22, all of solar cycle 23, and the early phase of solar cycle 24. This unprecedented long-term data set revealed that (1) the He^+/H^+ and O^+/H^+ flux ratios in the plasma sheet were dependent on the F10.7 index; (2) the F10.7 index dependence is stronger for O^+/H^+ than He^+/H^+; (3) the O^+/H^+ flux ratio is also weakly correlated with the ΣKp index; and (4) the He^{2+}/H^+ flux ratio in the plasma sheet appeared to show no long-term trend. From these results, we derived empirical equations related to plasma sheet ion composition and the F10.7 index, and estimated that the average plasma ion mass changes from ∼1.1 amu during solar minimum to ∼2.8 amu during solar maximum. In such a case, the Alfvén velocity during solar maximum decreases to ∼60% of the solar minimum value. Thus, physical processes in the plasma sheet are considered to be much different between solar minimum and solar maximum. We also compared long-term variation of the plasma sheet ion composition with that of the substorm occurrence rate, which is evaluated by the number of Pi2 pulsations. No correlation or negative correlation were found between them. This result contradicts the O^+ triggering substorm model, in which heavy ions in the plasma sheet increase the growth rate of the linear ion tearing mode and play an important role in localization and initiation of substorms. In contrast, O^+ ions in the plasma sheet may prevent occurrence of substorms.

1. Introduction

Ion composition is an important issue in terrestrial plasma environment. Plasma around the Earth predominantly consists of H^+, but it also includes other ion species such as O^+ and He^{2+}. Since these ions are heavier than H^+, even a small amount of them can modify the properties of the plasma. For instance, the mass density of plasma with 93% H^+ and 7% O^+ is about twice that of plasma with 100% H^+. In such a heavy plasma, the velocity of Alfvén waves decreases to ∼71% of that in 100% H^+ plasma. The Alfvén velocity represents a fundamental physical property of the plasma; thus, the decrease in the Alfvén velocity is expected to result in changes in a number of phenomena occurring in the terrestrial plasma. *Singer et al.* [1979] reported that periods of geomagnetic pulsations observed by geosynchronous satellites become consistent with model predictions when heavy plasma (i.e., 5∼9 amu (atomic mass unit)) is taken into account. *Nakamura et al.* [1995] performed numerical simulations of the slow shock for 1 amu plasma (100% H^+) and 1.3 amu plasma (98% H^+ and 2% O^+). They found that structures of the slow shock become different and an Alfvénic precursor preceded the slow shock in the latter case.

Moreover, heavy ions may also change physical processes during substorms, because of their large gyroradius. Adopting the growth rate of the linear ion tearing mode instability derived by *Schindler* [1974], which is proportional to the 3/2th power of the ion gyroradius, *Baker et al.* [1982] insisted that the existence of O^+ ions in the plasma sheet increases the growth rate of the linear ion tearing mode and makes favorable conditions for substorm occurrence. In a subsequent study, *Baker et al.* [1985] reported ISEE-1 observations of substorms that were consistent with this O^+ triggering substorm model. They also proposed a positive feedback mechanism of substorm triggering; that is, once a substorm occurs, mass-loading takes place by outflow of heavy ions from the ionosphere to the plasma sheet, and more favorable conditions for substorm triggering are established.

As shown above, ion composition has striking influences on various phenomena of the solar-terrestrial physics. From the viewpoint of space weather forecasting and space climate, we need to investigate how ion composition changes in the long term, for example, in the 11-year solar cycle. There are some previous studies examined ion composition changes near geosynchronous altitude and/or in the magnetotail. *Young et al.* [1982] examined the relation between the number density of heavy ions at L=6-7 and solar activity. In an analysis of ion flux data in the energy range of 0.9-15.9 keV from the GEOS-1 and -2 satellites, it was found that the He^+ and O^+ densities had a good correlation with the F10.7 index. *Stokholm et al.* [1989] also used data from GEOS-2 and reported results similar to those of *Young et al.* [1982]. Using the Polar satellite, *Pulkkinen et al.* [2001] examined variations of energetic (1-200 keV) ion composition at L=3-8 as a function of solar activity.

Their result showed that the He^+/H^+ and O^+/H^+ energy density ratios increase as solar activity increases. *Lennartsson* [1989] used ISEE-1 satellite data to study how ion composition in the plasma sheet (r=10-23 R_E) is controlled by solar activity. The He^+ and O^+ densities in the energy range of 0.1-16 keV were found to depend on the F10.7 index. These studies showed that the He^+ and O^+ densities (or energy densities) are correlated with the F10.7 index; however, the result was derived from a data set covering a period much shorter than one solar cycle, that is, 4.5 years for Young et al., 2.5 years for Pulkkinen et al., and 2 years for Lennartsson. Although Stokholm et al. used data covering 7 years, there was a data gap of ∼2 years (see their Figure 2), resulting in an available data period of ∼5 years. To confirm the solar activity dependence of ion composition, it is desirable to use long-term data covering longer than 11 years.

The Geotail spacecraft was launched on 24 July 1992, and is still operational as of March 2009. Figure 1 shows the orbit of the Geotail spacecraft after its launch in geocentric solar magnetospheric (GSM) coordinates. In the early phase, the spacecraft surveyed the distant tail of X_{GSM}=−50 R_E to −210 R_E. In the next phase, the spacecraft was maneuvered into an orbit with an apogee of ∼50 R_E [*Nishida*, 1994]. In March 1995, the apogee was lowered further, and Geotail was placed in near-Earth orbit having a perigee of 8-9 R_E, an apogee of 30 R_E, an orbital period of ∼5.3 days, and an apsidal period of ∼1 year. Geotail carries an instrument that can measure energetic ion flux with mass and charge state information. The energetic ion flux data were accumulated for more than 16 years without data gaps. It is unprecedented that energetic plasma data are obtained by a single spacecraft for such a long period. Thus, this unique data set makes it possible to investigate variations in the ion composition of the plasma sheet over one solar cycle for the first time.

The purpose of this paper is twofold. First, we analyze the Geotail data, examine variations in the ion composition during solar cycle 23 and longer, and estimate changes in the plasma ion mass in the plasma sheet. Second, comparing the ion composition in the plasma sheet with the occurrence of substorms, we argue a role for heavy ions in triggering substorms. The rest of the paper is as follows. In section 2, we describe the instrumentation and data set. Section 3 shows long-term variations in the ion composition, solar activity index, and geomagnetic index. Section 4 compares the plasma sheet ion composition and substorm occurrence rate which is evaluated by Pi2 pulsations. In section 5, we discuss the two issues raised above (i.e., changes in the average plasma ion mass and the role of heavy ions for substorm onset). Section 6 gives our conclusions.

2. Instrumentation and Data Set

2.1. Geotail/EPIC/STICS

We used the energetic ion flux data obtained by the suprathermal ion composition spectrometer (STICS) sensor of the energetic particle and ion composition (EPIC) instrument onboard the Geotail spacecraft [*Williams et al.*, 1994]. The STICS sensor measures the ion flux in the energy range of 9.4-212.1 keV/e with mass and charge state information. The energy range is scanned by eight energy steps evenly spaced in logarithmic scale, each of which has a narrow energy band (E_{i+1}/E_i∼1.56 and $\Delta E_i/E_i$∼0.023, where E_i is the center energy of the ith energy step and ΔE_i is the energy band width). The energy steps are varied every one spin (∼3 sec); thus, it takes ∼24 sec to obtain one complete energy spectrum. The sensor has an almost full (∼4π sr) directional coverage with six identical telescopes having polar angles of ±(0°-26.7°), ±(26.7°-53.3°), and ±(53.3°-80.0°) with respect to the spacecraft spin plane.

EPIC/STICS observations started on 17 October 1992. The latest data when this paper was prepared are for 21 February 2009. We used all of the available data ranging over ∼16.3 years, which cover the declining phase of solar cycle 22, all of solar cycle 23, and the early phase of solar cycle 24. Ion species examined in this study are H^+, He^+, O^+, and He^{2+}. We calculated the integral flux (I) for each ion species by the following equations:

$$I = \sum_{i=1}^{8} \left(\frac{1}{6} \sum_{j=1}^{6} J_{ij} \right) \cdot \Delta E_i', \quad (1)$$

$$\Delta E_i' = 0.44 E_i, \quad (2)$$

where J_{ij} is the spin-averaged differential flux measured at the ith energy step of the jth telescope. Within the parentheses of the first equation, the average differential flux over six telescopes is calculated. The factor of 0.44 in the second equation indicates that the energy band width used in this calculation ($\Delta E_i'$) is much wider than the actual energy band width (ΔE_i∼0.023E_i). The factor is decided such that energy ranges of two adjacent energy steps become continuous; in other words, E_i+$\Delta E_i'/2$ becomes equal to $E_{i+1}-\Delta E_{i+1}'/2$. We assumed that the observed differential flux (J_{ij}) is constant in the energy band of $E_i-\Delta E_i'/2$ to $E_i+\Delta E_i'/2$. According to the above equations, the calculated integral flux is for the energy range of 7.3-259 keV/e (i.e., 9.4−(0.44×9.4)/2 to 212.1+(0.44×212.1)/2 keV/e).

We checked whether the EPIC instrument was degraded during solar cycle 23 by comparing average spectra of ions in the region of X_{GSM}=−8∼−20 R_E, $|Y_{GSM}|\leq$8 R_E, and $|Z_{GSM}|\leq$3 R_E between 1997 and 2008, both of which are at solar minima. Both energy spectra were found to have similar shapes and be in the same flux level well within a factor of 2. Thus, we suppose that the EPIC instrument has had no significant degradation during its operation.

2.2. Surveying Region

Since we are interested in the terrestrial plasma environment, the surveying regions are limited to boxes labeled 1-3 with different colors (red, blue, and yellow) in Figure 1, where the plasma sheet is expected to be positioned. Regions 1-3 correspond to X_{GSM}=−8∼−20 R_E and $|Y_{GSM}|\leq$8 R_E, X_{GSM}=−20∼−32 R_E and $|Y_{GSM}|\leq$8 R_E, and X_{GSM}=−32∼−100 R_E and $|Y_{GSM}|\leq$14 R_E, respectively. A green curve designates the model magnetopause by *Shue et al.* [1997] with B_Z of 0 nT and a solar wind dynamic pressure of 1 nPa. In each surveying region, we calculated the 27-day average of the integral flux measured by Geotail/EPIC/STICS. The period of 27 days is selected because we want to eliminate effects of solar rotation, the period of which at the solar equator is about 27 days and to enhance statistical significance with data of ∼5 orbital periods (note that the orbital period of Geotail is ∼5.3 days). If the spacecraft entered or left the surveying region in the middle of a day, we ignored the data before the entry or after the leave. We also removed data in geomagnetic lobes where the calculated H^+ integral flux is zero.

2.3. Solar Activity Index and Geomagnetic Index

The daily F10.7 index was used to see solar activity. This index is derived from solar radio flux at a frequency of 2800 MHz (a wavelength of 10.7 cm) observed at local noon of Penticton, B.C., Canada; and is measured in solar flux units (sfu, 1 sfu=10^{-22} W/m^2/Hz). We used the F10.7 index for January 1992 to December 2008.

The Kp index was chosen to measure geomagnetic disturbances. Having a 3-hour time resolution, it has eight values in a day. In the following analysis, we used ΣKp which is a total of the eight Kp values. The ΣKp index was available for January 1992-February 2009.

For easy comparison with the Geotail/EPIC/STICS data, both indices were averaged over the 27-day period identical to that for the Geotail data.

3. Long-term Variation of Plasma Sheet Ion Composition

3.1. Integral Flux

Figures 2a and 2b show time profiles of X_{GSM} and Z_{GSM}, respectively, of the Geotail location after its launch. As mentioned

in section 1, Geotail surveyed the distant tail before spring 1995; thus, X_{GSM} varied in the range of $-210\ R_E$ to $20\ R_E$. After 1995, it was in a near-Earth orbit of 8-9 $R_E \times 30\ R_E$, resulting in periodical variations of X_{GSM}. Geotail has been operated to stay in the central plasma sheet (CPS) as long as possible before 2002; thus, Z_{GSM} has varied around $0\ R_E$. After 2002, however, such an operation was impossible because of the exhaustion of fuel for orbit control, leading to gradual orbital change in the negative Z direction. Figure 2b indicates that Geotail largely flew off the equatorial plane (Z_{GSM}=$-20\ R_E$ to $5\ R_E$) in 2007-2009, where the plasma sheet boundary layer (PSBL) and the magnetic lobe are more likely than the CPS.

Figures 2c-2f show the 27-day average of integral fluxes of H^+, He^+, O^+, and He^{2+}, respectively, for October 1992-February 2009. Data are designated as follows: region 1, red dots; region 2, blue dots; and region 3, yellow dots. All ion species have a jump in integral flux around 1995, followed by sinusoidal variations with a period of ∼1 year. These flux variations resemble those of X_{GSM} of Geotail location (Figure 2a). We found that the integral fluxes can generally be sorted by regions, being larger for region 1 and smaller for region 3. Therefore, such flux variations are due to a gradient of ion fluxes in the X_{GSM} direction. It can also be noted that the integral fluxes started to decrease slowly after 2002. We consider that this decrease is due to a change of Geotail position in Z_{GSM} (Figure 2b), because the ion fluxes in the PSBL and lobe are lower than those in the CPS. Therefore the observed integral fluxes strongly reflect the spatial distribution of energetic particles.

Nevertheless, it is worth noting that the O^+ integral flux shows an increasing trend clearly from 1995 to 2002, as found in Figure 2e. There is also a subtle increasing trend in the He^+ flux (Figure 2d), although no such trend seems to appear in the H^+ and He^{2+} fluxes (Figures 2c and 2f).

3.2. Integral Flux Ratio

To remove the effects of spatial distribution of ion fluxes in the X_{GSM} and Z_{GSM} directions, we calculated the ratio of the average integral flux of heavy ions to the average integral flux of H^+ (i.e., the integral flux ratio). Here the H^+ flux is chosen as a reference because it is a primary constituent of the plasma sheet plasma and appears to have no long-term trend (Figure 2c). The He^+/H^+, O^+/H^+, and He^{2+}/H^+ integral flux ratios are shown in Figures 3a-3c, respectively. The display format is the same as in Figures 2c-2f. The jumps or sinusoidal variations are no longer present. Figures 3d and 3e show the 27-day averages of the F10.7 and ΣKp indices, respectively. The F10.7 index distinctly indicates an 11-year solar cycle with minimum activity in 1995-1996 and 2008, and maximum activity in 2000-2001. The data period covers the declining phase of solar cycle 22, all of solar cycle 23, and the early phase of solar cycle 24. Geomagnetic activity does not show clear correlations with solar activity; ΣKp remained at a high level of 20-30 during the declining phases of F10.7 (1992-1994 and 2003-2005). This is consistent with the results of previous studies [e.g., *Ol'*, 1972; *Venkatesan et al.*, 1991; *Vennerstrøm and Friis-Christensen*, 1996].

In Figures 3a and 3b we found that the He^+/H^+ and O^+/H^+ integral flux ratios changed over a long timescale. They decreased gradually from 1993 to 1995 and stayed at minimum levels in 1996, followed by increases in 1997-2001. After peaks in late 2001, flux ratios started to decrease again. Minimum and maximum ratios were $\sim 1\times10^{-3}$ and $\sim 2\times10^{-3}$ for He^+/H^+, and $\sim 1\times10^{-2}$ and $\sim 5\times10^{-2}$ for O^+/H^+, indicating that the change in O^+/H^+ is larger than that in He^+/H^+. These long-term changes are well correlated with that of F10.7 rather than that of ΣKp. Furthermore, as indicated by arrows in Figures 3a, 3b, and 3d, small dents appeared in the He^+/H^+ and O^+/H^+ flux ratios in the middle of 2001 and they corresponded to a small decrease of the F10.7 index. Thus we conclude that both the He^+/H^+ and O^+/H^+ integral flux ratios are controlled by solar activity.

On the other hand, the He^{2+}/H^+ integral flux ratio demonstrated different features. It seems to stay at an almost constant level of 0.5×10^{-2}-1.0×10^{-2}. There is no similarity in time profile between the flux ratio and the indices. We believe that the He^{2+}/H^+ flux ratio is not correlated with solar activity.

3.3. Correlation Analysis Between Integral Flux Ratio and Indices

To confirm the results from Figure 3, correlation analysis was performed. Figure 4 shows how the integral flux ratios in regions 1 and 2 are related to the F10.7 and ΣKp indices for 1995-2009. From top to bottom, panels show the He^+/H^+, O^+/H^+, and He^{2+}/H^+ flux ratios, respectively. Left panels are against the F10.7 index, and right panels are against the ΣKp index.

Figures 4a and 4b indicate that the He^+/H^+ integral flux ratio is correlated well with the F10.7 index (correlation coefficient (c.c.) of 0.88), whereas it has no clear correlation with the ΣKp index (c.c.=0.35). The correlation coefficient between the O^+/H^+ integral flux ratio and the F10.7 index is also as high as 0.84 (Figure 4c). It seems from Figure 4d that the O^+/H^+ ratio is related to the ΣKp index (c.c.=0.57), but the coefficient is smaller than that for the F10.7 index. Because of the large correlation coefficients, we can draw linear regression lines in Figures 4a and 4c, which are expressed as

$$\log_{10}(R_{He^+/H^+}) = 0.00274 \times f_{F10.7} - 3.21, \quad (3)$$

$$\log_{10}(R_{O^+/H^+}) = 0.00651 \times f_{F10.7} - 2.50, \quad (4)$$

where R_{He^+/H^+} and R_{O^+/H^+} are the integral flux ratios of He^+/H^+ and O^+/H^+, and $f_{F10.7}$ is the F10.7 index. The slopes of these equations indicate that the O^+/H^+ ratio is more sensitive to solar activity than the He^+/H^+ ratio. Figures 4e and 4f indicate that the He^{2+}/H^+ integral flux ratio is not correlated with either the F10.7 or the ΣKp indices, as can be understood from correlation coefficients of 0.27 and 0.42. Thus, we substantiated the results found in section 3.2 (Figure 3); additionally, it was revealed that the O^+/H^+ ratio is weakly dependent on geomagnetic activity.

4. Long-term Variation of Substorm Occurrence Rate

4.1. Number of Pi2 Onsets

To examine whether the existence of heavy ions causes frequent occurrence of substorms as proposed by *Baker et al.* [1982, 1985], we compared long-term variations of ion composition in the plasma sheet with those of substorm occurrence rate. Here, the substorm occurrence rate is evaluated by the number of Pi2 pulsations observed at the Kakioka observatory (27.4° geomagnetic latitude, 208.8° geomagnetic longitude) at 2100-0100 magnetic local time (MLT). Pi2 pulsations were selected from 1-second geomagnetic field data by an automated detection program. This program applies wavelet analysis to the 1-second data and detects Pi2 pulsations with a peak-to-peak amplitude larger than 0.6 nT. The rate of successful detection is ∼94% for 2100-0100 MLT [*Nosé et al.*, 1998]. Details of the detection algorithm are described in *Nosé et al.* [1998, 2006]. The number of detected Pi2 pulsations was counted once every day (i.e., the daily number of Pi2) and averaged over 27-day intervals that are the same as in the Geotail/EPIC data.

Figures 5a and 5b display the He^+/H^+ and O^+/H^+ integral flux ratios, which are the same as Figures 3a and 3b, for easier comparison between ion composition and substorm occurrence rate. Figure 5c shows the 27-day average of the daily number of Pi2 pulsations appearing at Kakioka at 2100-0100 MLT. This daily number shows long-term variations between ∼1 and ∼5 with a minimum around 2000-2001 and maxima around 1994 and 2004. No clear correlation appears between the ion composition and the substorm occurrence rate.

4.2. Number of Pi2 Onsets Normalized by Solar Wind-Magnetosphere Coupling Function

In section 4.1, we compare between the ion composition and the substorm occurrence rate, but the substorm occurrence rate may depend on the amount of energy supplied from the solar wind to the

magnetosphere. Even if favorable conditions for substorm triggering are set in the magnetosphere, no substorm will occur if there is no energy supply from the solar wind. This idea leads us to normalize the substorm occurrence rate by the amount of energy from the solar wind. The energy is estimated by the solar wind-magnetosphere coupling function. Here we adopted Kan and Lee's electric field (ε) [*Kan and Lee*, 1979] as the coupling function, which is expressed as

$$\varepsilon = VB\sin^2\left(\frac{\theta}{2}\right), \quad (5)$$

where V is the solar wind velocity, B is the magnitude of the IMF, and θ is the polar angle of the IMF in the Y_{GSM}-Z_{GSM} plane. Variations in ε are shown in Figure 5d and each data point means an average value over the same 27-day interval. Figure 5e shows the result of normalization, that is, the daily number of Pi2 pulsations divided by ε. The normalized daily number of Pi2 pulsations also changes in the long term. It has peaks around 1996 and 2008 and a minimum around 2000-2001. Comparing Figure 5a (or 5b) with Figure 5e, we noticed that the correlation looks negative rather than positive.

4.3. Correlation Analysis Between Integral Flux Ratio and Number of Pi2 Onset

To confirm the above results, a correlation analysis was performed between the integral flux ratios and the daily number (or normalized daily number) of Pi2 pulsations. From Figures 6a and 6b, we see no clear correlation between the integral flux ratios and the daily number of Pi2 pulsations (c.c.=-0.29 and -0.20, respectively). However, as shown in Figures 6c and 6d, the normalized daily number of Pi2 is negatively correlated with the integral flux ratios (c.c.=-0.57 and -0.64), consistent with the result of section 4.2. Thus, we suppose that heavy ions may not play a crucial role in triggering substorms, but may prevent their occurrence.

5. Discussion

5.1. Variations in Plasma Sheet Ion Composition

With respect to the plasma sheet ion composition we found from Figures 2-4 that (1) the He^+/H^+ and O^+/H^+ flux ratios were dependent on the F10.7 index; (2) the F10.7 index dependence is stronger for O^+/H^+ than He^+/H^+; (3) the O^+/H^+ flux ratio is also weakly correlated with the ΣKp index; and (4) the He^{2+}/H^+ flux ratio appeared to show no long-term trend.

Let us begin by discussing results 1 and 2. It is well known that He^+ and O^+ in the plasma sheet originate in the ionosphere [e.g., *Shelley et al.*, 1972; *Chappell et al.*, 1987; *Moore*, 1991]. Although the F10.7 index is a direct measure of the 10.7 cm solar radio flux intensity, it is a good substitute for the solar UV/EUV irradiance as shown by *Floyd et al.* [2005], who reported c.c.=0.93 between F10.7 and Ly-α emission (121.6 nm) and c.c.=0.95 between F10.7 and He II emission (30.4 nm). Solar UV/EUV radiation is absorbed in the ionosphere and increases the ion density of He^+ and O^+ in the F region and the topside ionosphere [e.g., *Truhlík et al.*, 2005]. It also increases the ion temperature and corresponding scale height. Figure 7 gives vertical profiles of ion density calculated from empirical models by *Danilov and Smirnova* [1995] and *Třísková et al.* [2003] embedded in the International Reference Ionosphere 2007 [*Bilitza and Reinisch*, 2008]. Each panel shows the ion density of H^+ (thin line), He^+ (medium line), and O^+ (heavy line) at 00 LT at a geomagnetic latitude of 75° and geomagnetic longitude of 0° for three different solar activity levels, that is, solar minimum (April 1, 1997, left panel), the growth phase (April 1, 1999, middle panel), and solar maximum (April 1, 2001, right panel). As solar activity increases, the ion density increases and the distribution is shifted upwards, in particular, for O^+ ions. During solar minimum, ion density at 2000 km altitude is 3.74×10^2 cm^{-3} for H^+, 3.80 cm^{-3} for He^+, and less than 0.10 cm^{-3} for O^+ (the O^+ density is too small and outside the range to which the model is applicable). However, during solar maximum, ion density at the same altitude increases to 7.26×10^2 cm^{-3} for H^+, 59.1 cm^{-3} for He^+, and 17.1 cm^{-3} for O^+, resulting in a rate of increase of 1.9 for H^+, 15.6 for He^+, and larger than 171 for O^+. Ions in the topside ionosphere will further accelerate and flow out from the Earth to the magnetosphere. Thus, the above model predicts that the amount of O^+ ions supplied to the magnetosphere will drastically increase during solar maximum, whereas that of He^+ ions will increase a little and that of H^+ will have almost no change. Such features have been observed by satellites at high altitude (8000 to 23000 km altitude) [*Yau et al.*, 1985a, 1988]. Thus, results 1 and 2 can be explained by the above scenario.

Strangeway et al. [2005] proposed two primary energy sources of ion outflow in a rather short timescale (about a few hours): downward Poynting flux and soft electron precipitation. The former would cause ion upwelling via Joule dissipation at the lower ionosphere, whereas the latter would cause ion upwelling through the ambipolar electric field that accompanies ionospheric electron heating at high altitudes. The upwelling ions need to be further accelerated by transverse electromagnetic waves to escape from the ionosphere. Both energy sources increase in a geomagnetically disturbed condition; thus, we can expect many O^+ ions to escape from the ionosphere to the magnetosphere during periods of large Kp. This expectation is confirmed by previous satellite observations showing a good correlation between O^+ outflow flux and the Kp (or Dst) index [e.g., *Yau et al.*, 1985b, 1988; *Abe et al.*, 1996]. Therefore we found another correlation between O^+ flux in the plasma sheet and ΣKp (result 3).

He^{2+} originates in the solar wind [*Bochsler*, 1987]. *Bame et al.* [1983] and *Ogilvie et al.* [1989] compiled long-term averages of the He^{2+} abundance (i.e., He^{2+}/H^+) in the solar wind reported by previous studies. They found that the He^{2+} abundance follows solar activity, though its variation is as small as a factor of ∼1.6. This variation factor may be too small to resolve with the EPIC observations. These features of the solar wind ion composition may be the reason Geotail observed a rather constant ratio of He^{2+}/H^+ in the plasma sheet (result 4).

5.2. Estimation of Plasma Ion Mass

One of the purposes of this study was to find how the plasma ion mass in the plasma sheet changes during a solar cycle. From Figures 4a and 4c we revealed that the integral flux ratio is strongly controlled by the F10.7 index and derived empirical equations between them (equations 3 and 4). Using these equations, we can estimate the typical ion composition in a plasma sheet. However, one may argue that the equations give the integral flux ratios in the high energy range of 7.3-259 keV/*e*, and the computed values do not represent number density ratios of He^+/H^+ and O^+/H^+. To examine this argument, we investigated changes of energy spectra during the growth phase of solar cycle 23. The left panel of Figure 8 illustrates energy spectra of H^+ ions in region 1 in 1996 (open circles), 1998 (open triangles), 2000 (filled circles), and 2002 (filled triangles); the middle and right panels show He^+ and O^+ ions. The energy spectra of H^+ do not show any significant changes, whereas the differential fluxes of He^+ and O^+ ions are enhanced overall, and their spectral shapes are almost unaltered. This implies that the differential flux of He^+ and O^+ ions at energies lower than 7.3 keV was also increased during solar maximum. Because of these features of the energy spectra, we may assume that the integral flux ratios estimated from equations 3 and 4 reflect the density ratios.

When $f_{F10.7}$=50 sfu and $f_{F10.7}$=250 sfu were taken as typical values of the F10.7 index at solar minimum and solar maximum, respectively, the empirical equations give $R_{He^+/H^+}=10^{-3.07}=8.51\times10^{-4}$ and $R_{O^+/H^+}=10^{-2.17}=0.00676$ for solar minimum, and $R_{He^+/H^+}=10^{-2.53}=0.00295$ and $R_{O^+/H^+}=10^{-0.87}=0.135$ for solar maximum. These flux ratios can be regarded as density ratios, and then we derive a plasma ion mass of 1.10 amu for solar minimum and 2.79 amu for solar maximum. If we consider a contribution of He^{2+} ($R_{He^{2+}/H^+}\sim1\times10^{-2}$), the plasma ion mass

becomes 1.13 amu for solar minumum and 2.80 amu for solar maximum. These results indicate that the plasma in the plasma sheet consists mostly of protons during solar minimum, and that it becomes nearly 2.5 times as heavy as the proton plasma during solar maximum. Moreover, using these results to calculate the Alfvén velocity, we found that the Alfvén velocity during solar maximum decreases to ∼60% of that during solar minimum. Since the Alfvén velocity is one of the primary parameters in the plasma, physical processes in the magnetosphere and plasma sheet are expected to differ greatly between solar minimum and solar maximum.

5.3. Role of Heavy Ions in Substorm Triggering

Baker et al. [1982, 1985] proposed the O^+ triggering substorm model, where heavy ions in the plasma sheet increase the growth rate of the linear ion tearing mode, playing an important role in the localization and initiation of substorms. However, *Lennartsson et al.* [1993] analyzed the ISEE-1 and AMPTE/CCE data statistically, and argued that O^+ ions have no destabilizing effects on the plasma sheet. The controversy continues in the study by *Daglis and Sarris* [1998], which rebutted the argument of Lennartsson et al. and considered O^+ ions as a catalytic agent of magnetospheric activity. *Kistler et al.* [2006] could not find the expected effects of O^+ of decreasing the threshold of substorm onset from the Cluster data and stated that a triggering mechanism other than ion tearing mode instability may be responsible. As shown above, the discussion regarding the O^+ triggering substorm model is tangled, and a new approach from a different point of view is needed to unravel the role of O^+ ions.

In the present study we intended to tackle this issue by comparing the ion composition in the plasma sheet with the substorm occurrence rate throughout ∼16 years. Figures 6a and 6b showed no clear correlations between the integral flux ratios and the daily number of Pi2 pulsations (c.c.=−0.2∼−0.3). When the daily number of Pi2 pulsations is normalized by Kan and Lee's electric field, the correlation coefficients become negatively larger and have values of −0.6∼−0.65 (Figures 6c and 6d), implying that heavy ions tend to prevent occurrence of substorms. Thus the result seems to be against the model of *Baker et al.* [1982, 1985]. *Shay and Swisdak* [2004] examined the effect of O^+ ions on the reconnection rate in the magnetotail, using both linear analysis and numerical simulation. They found that O^+ ions reduce the speed of downstream plasma flow and thus makes the reconnection rate small. This indicates that either the substorm expansion phase takes a longer time or less of the lobe field reconnects in an O^+-rich plasma. If the small reconnection rate causes a decrease in the number of substorm occurrences, the result in the present study may support the model proposed by *Shay and Swisdak* [2004].

6. Summary

We examined long-term variations of ion composition in the plasma sheet, using the energetic (9.4-212.1 keV/*e*) ion flux data obtained by the EPIC/STICS instrument onboard the Geotail spacecraft. Data coverage is from 17 October 1992 to 21 February 2009, ranging over ∼16.3 years. This is an unprecedentedly long-term observation by a single instrument. It was found that (1) the abundance of ionospheric ions (He^+/H^+ and O^+/H^+) depends on the solar activity; (2) this dependence is strong in case of O^+ ions; (3) the O^+ abundance also weakly depends on geomagnetic activity; and (4) the abundance of solar wind ions (He^{2+}/H^+) has no correlation with both the solar activity and the geomagnetic activity.

From the above results, we derived empirical equations relating the plasma sheet ion composition and the F10.7 index. The equations estimate the plasma ion mass during solar minimum as ∼1.1 amu and that during solar maximum as ∼2.8 amu. This indicates that the Alfven velocity during solar maximum decreases to ∼60% of that during solar minimum. Since the Alfven velocity is one of the primary parameters in plasma, physical processes in the plasma sheet are expected to differ greatly different between solar minimum and solar maximum.

We compared the long-term changes between the plasma sheet ion composition and occurrence rate of substorms. The substorm occurrence rate is estimated by the number of Pi2 pulsations or the number of Pi2 normalized by the solar wind-magnetosphere coupling function (Kan and Lee's electric field). We found no clear correlation or negative correlation between ion composition and substorm occurrence rate. This result indicates that heavy ions do not play a crucial role in triggering substorms, but rather prevent their occurrence.

Appendix

The Geotail satellite is still in operation, and the EPIC/STICS instrument is working well as of March 2009. Thus, Figures 2-6 can be updated in future. Updated figures are available from the web site (http://wdc.kugi.kyoto-u.ac.jp/~nose/public).

Acknowledgements

We thank D. J. Williams, R. W. McEntire, A. T. Y. Lui, and S. R. Nylund for their help in processing the Geotail/EPIC data. The Kp index was provided by H.-J. Linthe at Helmholtz Centre Potsdam, GFZ German Research Centre for Geosciences. The F10.7 index was provided by Penticton, B.C., Canada through the NOAA/NGDC SPIDR (Space Physics Interactive Data Resource) WWW site. We are thankful to S. Machida for his helpful comments. This work was supported by the Kurata Memorial Hitachi Science and Technology Foundation (grant 844), the Japan Securities Scholarship Foundation (grant 1368), Inamori Foundation, and the Ministry of Education, Science, Sports and Culture, Grant-in-Aid for Young Scientists (B) (grant 17740327 and 19740303).

References

Abe, T., S. Watanabe, B. A. Whalen, A. W. Yau, and E. Sagawa (1996), Observations of polar wind and thermal ion outflow by Akebono/SMS, *J. Geomagn. Geoelectr.*, *48*, 319–325.

Baker, D. N., E. W. Hones, Jr., D. T. Young, and J. Birn (1982), The possible role of ionospheric oxygen in the initiation and development of plasma sheet instabilities, *Geophys. Res. Lett.*, *9*(12), 1337–1340, doi:10.1029/GL009i012p01337.

Baker, D. N., T. A. Fritz, J. Birn, W. Lennartsson, B. Wilken, and H. W. Kroehl (1985), The role of heavy ionospheric ions in the localization of substorm disturbances on March 22, 1979 - CDAW 6, *J. Geophys. Res.*, *90*(A2), 1273–1281, doi:10.1029/JA090iA02p01273.

Bame, S. J., W. C. Feldman, T. J. Gosling, D. T. Young, and R. D. Zwickl (1983), What Magnetospheric Workers Should Know about Solar Wind Composition, in *Energetic Ion Composition in the Earth's Magnetosphere*, edited by R. G. Johnson, pp. 73–98, Terra Scientific Pub., Tokyo.

Bilitza, D., and B. W. Reinisch (2008), International Reference Ionosphere 2007: Improvements and new parameters, *Adv. Space Res.*, *42*, 599–609, doi:10.1016/j.asr.2007.07.048.

Bochsler, P. (1987), Solar wind ion composition, *Physica Scripta Volume T*, *18*, 55–60.

Chappell, C., T. Moore, and J. W. Jr. (1987), The ionosphere as a fully adequate source of plasma for the Earth's magnetosphere, *J. Geophys. Res.*, *92*(A6), 5896–5910, doi:10.1029/JA092iA06p05896.

Daglis, I. A., and E. T. Sarris (1998), Comment on "Experimental investigation of possible geomagnetic feedback from energetic (0.1 to 16 keV) terrestrial O^+ ions in the magnetotail current sheet" by O. W. Lennartsson, D. M. Klumpar, E. G. Shelley and J. M. Quinn, *J. Geophys. Res.*, *103*(A12), 29,545–29,548, doi:10.1029/98JA02268.

Danilov, A. D., and N. V. Smirnova (1995), Improving the 75 to 300 km ion composition model of the IRI, *Adv. Space Res.*, *15*(2), 171–177, doi:10.1016/S0273-1177(99)80044-1.

Floyd, L., J. Newmark, J. Cook, L. Herring, and D. McMullin (2005), Solar EUV and UV spectral irradiances and solar indices, *J. Atmos. Solar-Terr. Phys.*, *67*, 3–15, doi:10.1016/j.jastp.2004.07.013.

Kan, J. R., and L. C. Lee (1979), Energy coupling function and solar wind-magnetosphere dynamo, *Geophys. Res. Lett.*, *6*(7), 577–580, doi:10.1029/GL006i007p00577.

Kistler, L. M., et al. (2006), Ion composition and pressure changes in storm time and nonstorm substorms in the vicinity of the near-Earth neutral line, *J. Geophys. Res.*, *111*, A11222, doi:10.1029/2006JA011939.

Lennartsson, O. W., D. M. Klumpar, E. G. Shelley, and J. M. Quinn (1993), Experimental investigation of possible geomagnetic feedback from energetic (0.1 to 16 keV) terrestrial O^+ ions in the magnetotail current sheet, *J. Geophys. Res.*, *98*(A11), 19,443–19,454, doi:10.1029/93JA01991.

Lennartsson, W. (1989), Energetic (0.1- to 16-keV/e) magnetospheric ion composition at different levels of solar F10.7, *J. Geophys. Res.*, *94*(A4), 3600–3610, doi:10.1029/JA094iA04p03600.

Moore, T. E. (1991), Origins of magnetospheric plasma, *Rev. Geophys.*, *29*, 1039–1048.

Nakamura, M. S., M. Fujimoto, and K. Maezawa (1995), The effects of heavy ions on the slow shocks in the geomagnetotail, *J. Geophys. Res.*, *100*(A11), 21,843–21,856, doi:10.1029/95JA02101.

Nishida, A. (1994), The GEOTAIL mission, *Geophys. Res. Lett.*, *21*, 2871–2874.

Nosé, M., T. Iyemori, M. Takeda, T. Kamei, D. K. Milling, D. Orr, H. J. Singer, E. W. Worthington, and N. Sumitomo (1998), Automated detection of Pi2 pulsations using wavelet analysis: 1. Method and an application for substorm monitoring, *Earth, Planets, and Space*, *50*, 773–783.

Nosé, M., et al. (2006), Automated detection of Pi2 pulsations to monitor substorm signatures: its application to real-time data and archived data, *Proceedings Int. Conf. Substorms-8*, pp. 209–214.

Ogilvie, K. W., M. A. Coplan, P. Bochsler, and J. Geiss (1989), Solar wind observations with the ion composition instrument aboard the ISEE-3/ICE spacecraft, *Solar Phys.*, *124*, 167–183, doi:10.1007/BF00146526.

Ol', A. I. (1972), Physics of the 11-Year Variation of Magnetic Disturbances, *Geomagnetism and Aeronomy*, *11*, 549–551.

Pulkkinen, T. I., et al. (2001), Ring current ion composition during solar minimum and rising solar activity: Polar/CAMMICE/MICS results, *J. Geophys. Res.*, *106*(A9), 19,131–19,148, doi:10.1029/2000JA003036.

Schindler, K. (1974), A theory of the substorm mechanism., *J. Geophys. Res.*, *79*(19), 2803–2810, doi:10.1029/JA079i019p02803.

Shay, M. A., and M. Swisdak (2004), Three-Species Collisionless Reconnection: Effect of O^+ on Magnetotail Reconnection, *Physical Review Letters*, *93*(17), 175001, doi:10.1103/PhysRevLett.93.175001.

Shelley, E. G., R. G. Johnson, and R. D. Sharp (1972), Satellite Observations of Energetic Heavy Ions during a Geomagnetic Storm, *J. Geophys. Res.*, *77*(31), 6104–6110, doi:10.1029/JA077i031p06104.

Shue, J.-H., J. K. Chao, H. C. Fu, C. T. Russell, P. Song, K. K. Khurana, and H. J. Singer (1997), A new functional form to study the solar wind control of the magnetopause size and shape, *J. Geophys. Res.*, *102*(A5), 9497–9512, doi:10.1029/97JA00196.

Singer, H. J., C. T. Russell, M. G. Kivelson, T. A. Fritz, and W. Lennartsson (1979), Satellite observations of the spatial extent and structure of Pc 3, 4, 5 pulsations near the magnetospheric equator, *Geophys. Res. Lett.*, *6*(11), 889–892, doi:10.1029/GL006i011p00889.

Stokholm, M., H. Balsiger, J. Geiss, H. Rosenbauer, and D. T. Young (1989), Variations of the magnetospheric ion number densities near geostationary orbit with solar activity, *Ann. Geophys.*, *7*(1), 69–76.

Strangeway, R. J., R. E. Ergun, Y. J. Su, C. W. Carlson, and R. C. Elphic (2005), Factors controlling ionospheric outflows as observed at intermediate altitudes, *J. Geophys. Res.*, *110*, A03221, doi:10.1029/2004JA010829.

Truhlík, V., L. Trísková, and J. Šmilauer (2005), Manifestation of solar activity in the global topside ion composition – a study based on satellite data, *Ann. Geophys.*, *23*, 2511–2517.

Tŕísková, L., V. Truhlík, and J. Šmilauer (2003), An empirical model of ion composition in the outer ionosphere, *Adv. Space Res.*, *31*(3), 653–663, doi:10.1016/S0273-1177(03)00040-1.

Venkatesan, D., A. G. Ananth, H. Graumann, and S. Pillai (1991), Relationship between solar and geomagnetic activity, *J. Geophys. Res.*, *96*(A6), 9811–9813, doi:10.1029/90JA02322.

Vennerstrøm, S., and E. Friis-Christensen (1996), Long-term and solar cycle variation of the ring current, *J. Geophys. Res.*, *101*(A11), 24,727–24,736, doi:10.1029/96JA02178.

Williams, D. J., R. W. McEntire, C. Schlemm II, A. T. Y. Lui, G. Gloeckler, S. P. Christon, and F. Gliem (1994), Geotail energetic particles and ion composition instrument, *J. Geomagn. Geoelectr.*, *46*, 39–57.

Yau, A. W., P. H. Beckwith, W. K. Peterson, and E. G. Shelley (1985a), Long-term (solar cycle) and seasonal variations of upflowing ionospheric ion events at DE 1 altitudes, *J. Geophys. Res.*, *90*(A7), 6395–6407, doi:10.1029/JA090iA07p06395.

Yau, A. W., E. G. Shelley, W. K. Peterson, and L. Lenchyshyn (1985b), Energetic auroral and polar ion outflow at DE 1 altitudes: Magnitude, composition, magnetic activity dependence, and long-term variations, *J. Geophys. Res.*, *90*(A9), 8417–8432.

Yau, A. W., W. K. Peterson, and E. G. Shelley (1988), Quantitative parameterization of energetic ionospheric ion outflow, in *Modeling Magnetospheric Plasma*, *Geophys. Monogr. Ser.*, vol. 44, edited by T. E. Moore and J. J. H. Waite, pp. 211–217, AGU, Washington, D.C.

Young, D. T., H. Balsiger, and J. Geiss (1982), Correlations of magnetospheric ion composition with geomagnetic and solar activity, *J. Geophys. Res.*, *87*(A11), 9077–9096, doi:10.1029/JA087iA11p09077.

S. P. Christon, Focused Analysis and Research, Columbia, MD 21044, USA.

A. Ieda, Solar-Terrestrial Environment Laboratory, Nagoya University, Furo-cho, Chikusa-ku, Nagoya, Aichi 464-8601, Japan.

M. Nosé, Data Analysis Center for Geomagnetism and Space Magnetism, Graduate School of Science, Kyoto University, Oiwake-cho, Kitashirakawa, Sakyo-ku, Kyoto 606-8502, Japan. (nose@kugi.kyoto-u.ac.jp)

Figure 1. Orbit of the Geotail spacecraft in geocentric solar magnetospheric (GSM) coordinates for 17 October 1992 to 21 February 2009. Surveying regions are indicated by boxes labeled 1-3 with different colors (red, blue, and yellow). Regions 1-3 correspond to X_{GSM}=−8∼−20 R_E and $|Y_{GSM}|\leq$8 R_E, X_{GSM}=−20∼−32 R_E and $|Y_{GSM}|\leq$8 R_E, and X_{GSM}=−32∼−100 R_E and $|Y_{GSM}|\leq$14 R_E, respectively. A green curve designates the model magnetopause.

Figure 2. Geotail location in (a) X_{GSM} coordinates and (b) Z_{GSM} coordinates for October 1992-February 2009. Integral fluxes averaged over 27 days of (c) H^+, (d) He^+, (e) O^+, and (f) He^{2+} for October 1992-February 2009. Data are designated as follows: region 1, red dots; region 2, blue dots; and region 3, yellow dots.

Figure 3. Ratios of the 27-day average integral flux of (a) He^+/H^+, (b) O^+/H^+, and (c) He^{2+}/H^+ ions for October 1992-February 2009. Red, blue, and yellow dots correspond to region 1, 2, and 3, respectively. (d) F10.7 index averaged over 27 days. (e) ΣKp index averaged over 27 days. Vertical arrows indicate simultaneous occurrence of small decreases in the He^+/H^+ and O^+/H^+ flux ratios and the F10.7 index in the middle of 2001.

Figure 4. Relation between the He^+/H^+ flux ratio and (a) the F10.7 index and (b) the ΣKp index for 1995-2009. (c-d) Same as Figures 4a and 4b, except for O^+/H^+. (e-f) Same as Figures 4a and 4b, except for He^{2+}/H^+.

Figure 5. Integral flux ratios of (a) He^+/H^+ and (b) O^+/H^+, which are identical to Figures 3a and 3b. (c) Daily number of Pi2 pulsations appearing at Kakioka at 2100-0100 MLT. The number is averaged over 27 days. (d) Kan and Lee's electric field (ε) averaged over 27 days, which is adopted as the solar wind-magnetosphere coupling function. This electric field is calculated by $\varepsilon = VB\sin^2(\theta/2)$. (e) Normalized daily number of Pi2 pulsations, that is, the daily number of Pi2 pulsations divided by ε.

Figure 6. Relation between the daily number of Pi2 pulsations and (a) the He^+/H^+ flux ratio and (b) the O^+/H^+ flux ratio for 1995-2009. (c-d) Same as Figures 6a and 6b, except for the normalized daily number of Pi2 pulsations.

Figure 7. Vertical profiles of ion density at a local midnight at high latitude, which are calculated from empirical models by *Danilov and Smirnova* [1995] and *Třísková et al.* [2003] in the International Reference Ionosphere 2007. Each panel shows ion density for three different solar activity levels (solar minimum on the left, the growth phase in the middle panel, and solar maximum on the right).

Figure 8. Energy spectra of H^+, He^+, and O^+ ions in region 1 in 1996 (open circles), 1998 (open triangles), 2000 (filled circles), and 2002 (filled triangles).

Figure 1

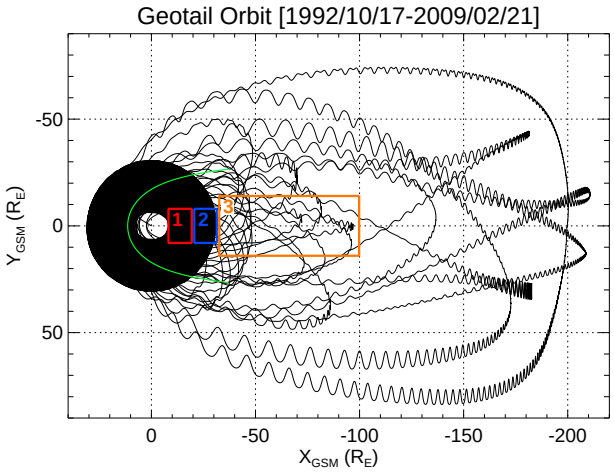

Figure 2

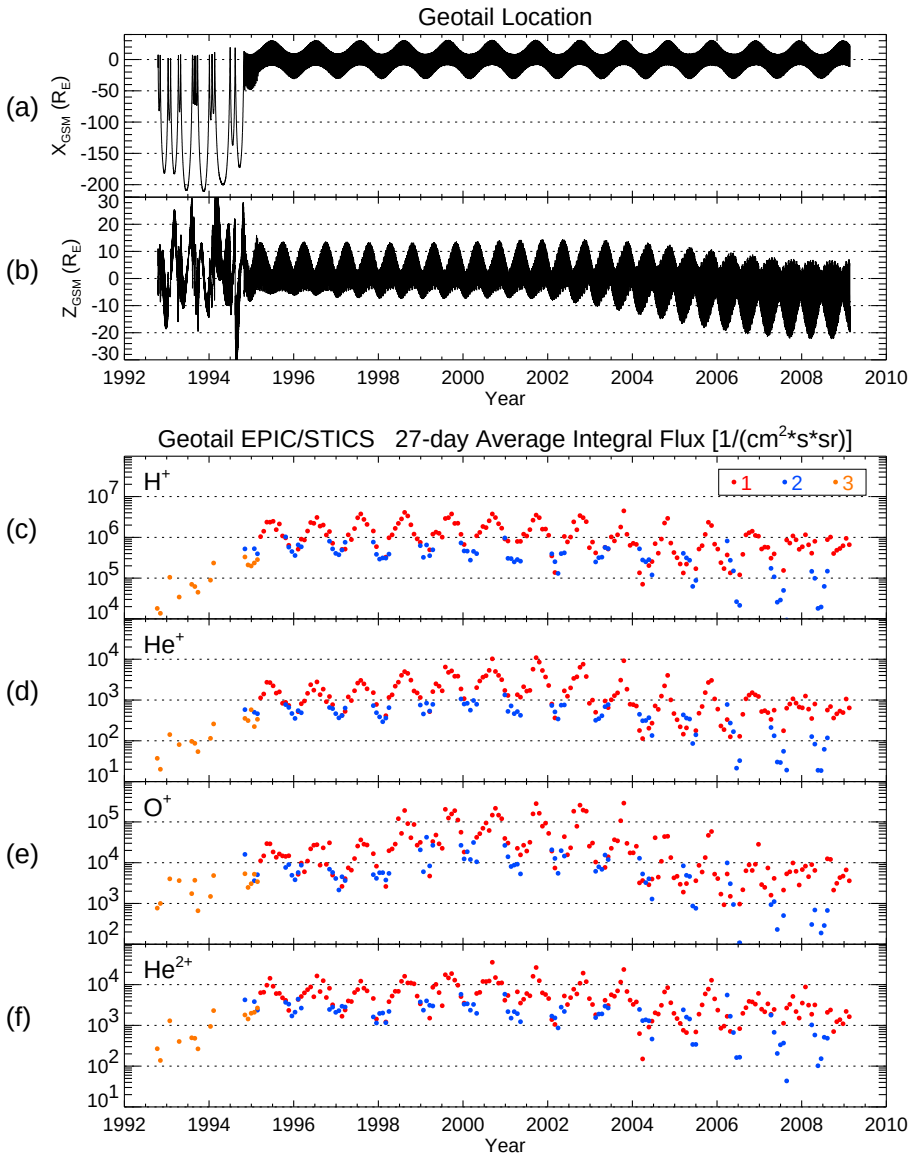

Figure 3

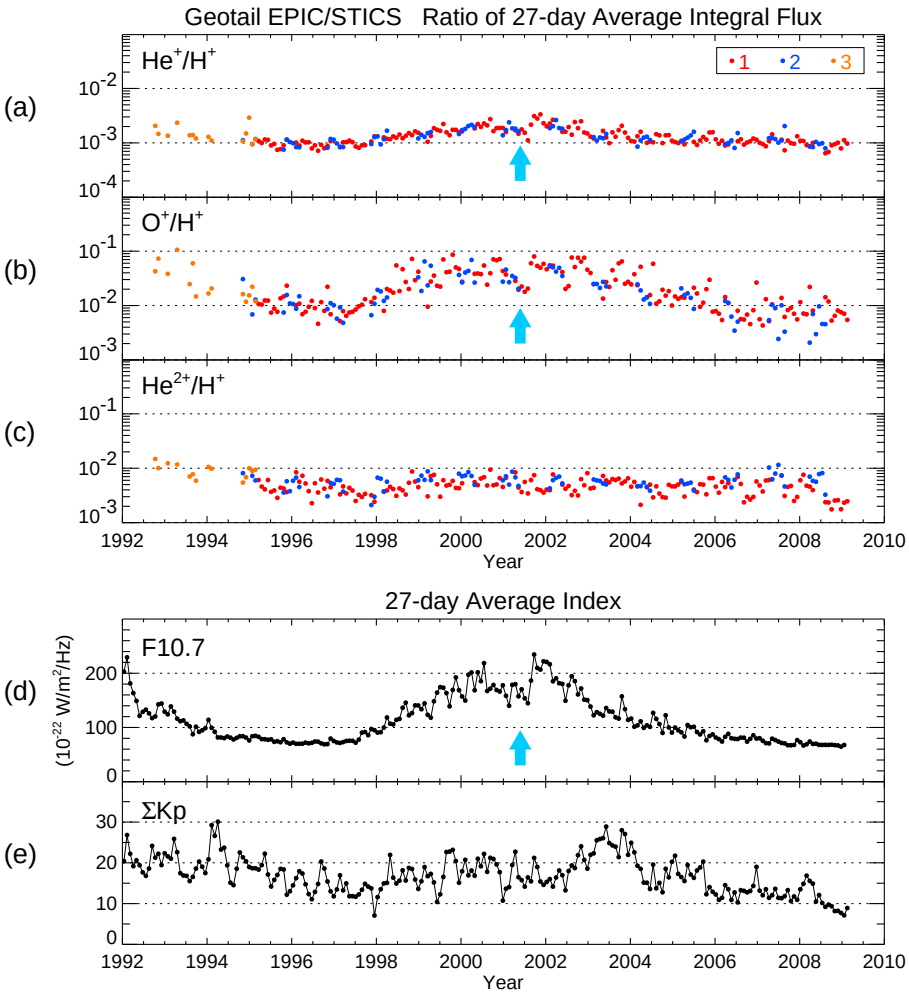

Figure 4

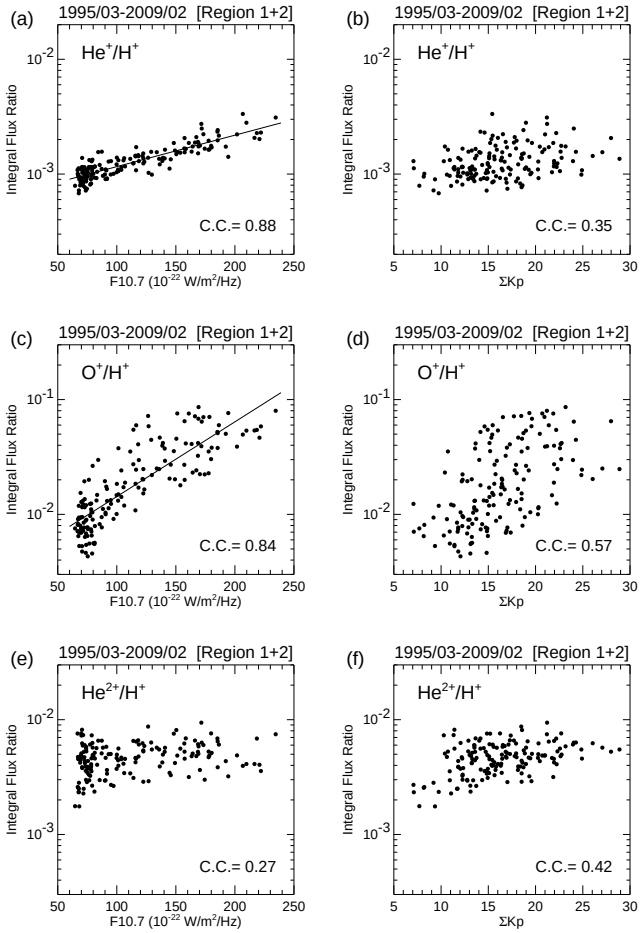

Figure 5

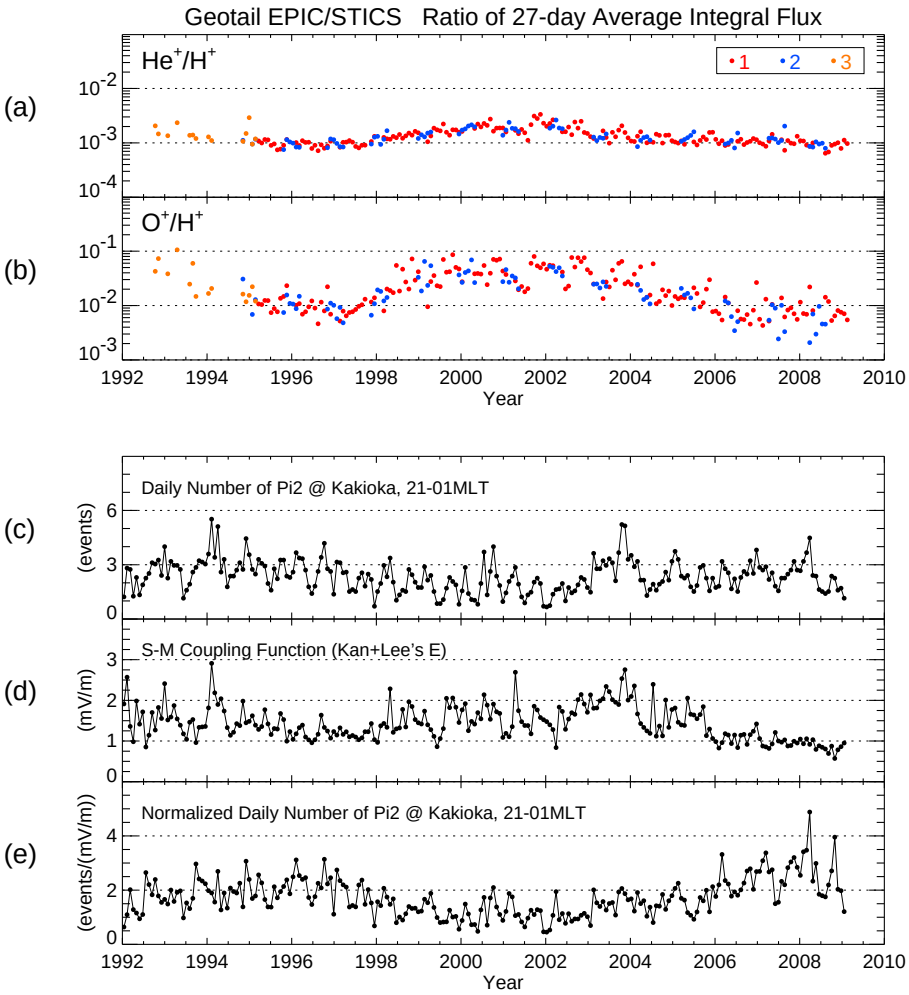

Figure 6

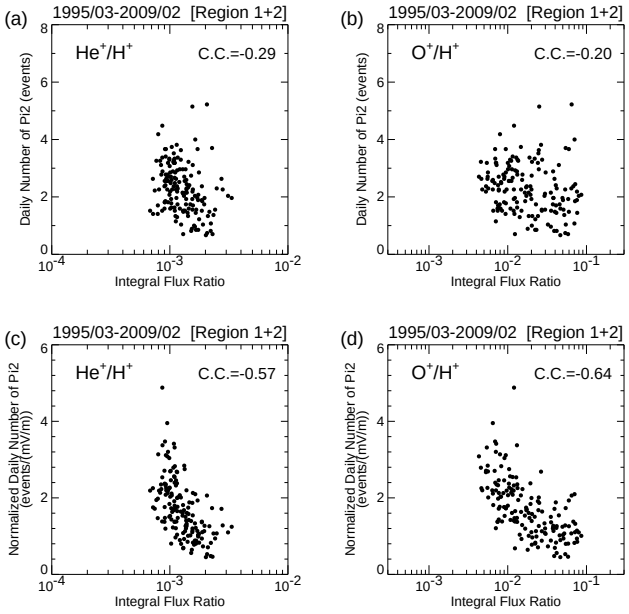

Figure 7

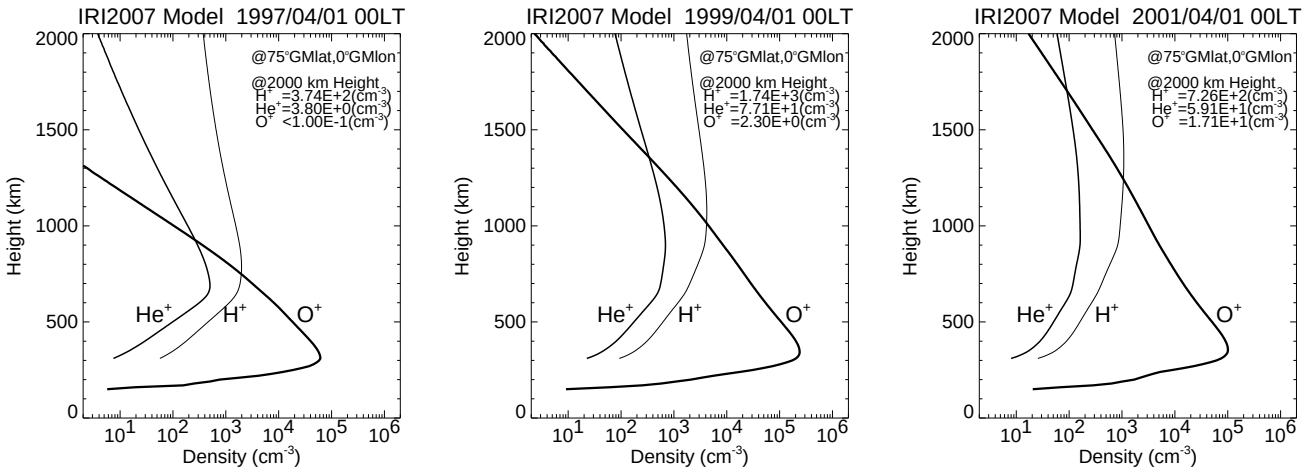

Figure 8